Available online at www.CivileJournal.org

Civil Engineering Journal

(E-ISSN: 2476-3055; ISSN: 2676-6957)

Vol. 12, No. 01, January, 2026

Numerical Analysis of Lateral and Vertical Deformation of the Embedded Length of Monopile in a Sandy Soil

Fatema S. Noori [1], Ghusoon S. Al-Qaisee [1*], Zainab M. Mohsin [1]

[1] *Technical Engineering Collage, Middle Technical University, Baghdad, Iraq.*

Received 01 March 2025; Revised 25 November 2025; Accepted 11 December 2025; Published 01 January 2026

Abstract

A monopile is a large-diameter steel cylinder partially inserted into seabeds; thus, it is one of the major selections of offshore wind and tower foundations. This study aimed to investigate the effect of monopile diameter, thickness, and ratio of soil embedded depth to height of water on the lateral and vertical displacements of the embedded part of the pile. In the study, the monopile was subjected to a lateral displacement equivalent to 10% of the pile diameter at the pile head in order to examine the lateral and vertical deformations of the embedded length of the pile. The three-dimensional finite element software PLAXIS 3D was used to simulate the study. The soil layer used consisted of one layer of medium-dense sandy soil. The study involved investigating the location along the embedded depths that exhibit zero lateral and vertical displacements; that location was found to depend on the monopile diameter, wall thickness, and ratio of embedded depth to water height. The depth of zero lateral displacement was found to increase as pile rigidity and wall thickness increase. The study shows that increasing the L/H ratio on the embedded depth of zero lateral displacement, L_{Hzero}, diminishes with increasing monopile diameter for the same wall thickness. Also, the variation of lateral displacement along pile length demonstrates a constant trend behavior regardless of pile thicknesses and diameters, but the depth of zero lateral displacement, L_{Hzero}, was varied. Furthermore, the monopile diameter effect on the vertical displacement shows that as the monopile diameter increases, the depth of zero vertical displacement decreases. Also, as L/H decreased, the depth of zero vertical displacement declined.

Keywords: Monopile Diameter; Monopile Wall Thickness; Monopile Embedded Depth; Monopile Embedded Depth; Depth of Zero Lateral and Vertical Displacements.

1. Introduction

In order to achieve a more effective approach to addressing climate change, it is essential to reduce carbon dioxide emissions, extend the lifespan of energy production, and minimize the depletion of available resources. Consequently, renewable energy sources have been widely adopted across the globe. Renewable energy is a major energy source and can be considered an alternative to traditional methods of energy generation. It provides many economic and environmental advantages. Worldwide, it is intended to obtain about 35% of electricity demand from renewable sources. Wind energy is considered one of the most efficient forms of renewable energy. Many offshore wind farms have been constructed or are planned offshore; therefore, a robust foundation with sufficient stiffness is required to resist unacceptable soil deformation or structural rotation [1, 2].

Monopile foundations are one of the efficient solutions for offshore wind structures. Such piles are suitable for towers and wind turbines in offshore environments, since piles with large diameters can be successfully installed for

* Corresponding author: ghussadiq@mtu.edu.iq

https://doi.org/10.28991/CEJ-2026-012-01-023

such structures. A monopile usually consists of a large-diameter steel cylinder partially embedded in the seabed. Many studies have shown that monopiles can satisfy the required safety demands, as such steel piles are easy to construct with diameters up to 8 m and lengths up to 80 m, with embedded depths up to 10 times the pile diameter [3, 4].

Usually, there are four stages in monopile construction: onshore manufacturing, loading at the port, transportation, and offshore installation. Two design criteria must be considered when designing piles to resist lateral loads: providing a safety factor by reducing the ultimate load and ensuring an allowable lateral displacement. Generally, designing based on allowable lateral displacement is considered a more logical approach, since it allows the designer to address both the ultimate bearing capacity state and the serviceability limit state [5].

Higgins et al. [6] used Fourier FEM to analyze laterally loaded piles embedded in various elastic soils. In their study, piles with different lengths, flexibilities, and boundary conditions were first embedded in a single layer with constant and linearly varying modulus, and then in a two-layer system with constant modulus within each layer. A set of algebraic equations was developed to describe pile head deflection, rotation, and bending moment by fitting the results of the FE analyses.

Haiderali et al. [7] studied the behavior of monopiles installed in undrained clayey soil under axial and lateral loads using three-dimensional finite element analysis. Their study examined four piles, each 35 m long, with diameters varying from 4 to 7.5 m. Their results showed that under lateral loading, monopiles deformed mainly due to rotation about a pivot point, while the pile toes experienced negative displacement. The effect of axial load on the ultimate lateral capacity or lateral displacement of monopiles was insignificant.

Kozubal et al. [2] conducted a study using a 3D probabilistic approach to analyze pile displacement under lateral loads. They focused on a single pile subjected to lateral loads, considering several typical subsurface models. Initially, a random modulus of elasticity was assigned to each layer of a multi-layer linear elastic soil. Subsequently, a model of linear elastic soil with a modulus of elasticity increasing randomly with depth was investigated. Their findings showed that the reliability indices, used to evaluate the suitability of pile design under specific subsurface conditions, were influenced by the random variability of both the lateral force and the modulus of the upper soil layer.

Lada et al. [8] focused on the analysis of a large-diameter monopile using a numerical analysis model. Pile diameter, pile length, and load eccentricity were investigated. The results showed that pile diameter and soil properties have the greatest effect on the ultimate soil bearing capacity, while load eccentricity has a lesser effect. The deformation pattern varies according to pile stiffness or slenderness, where stiff piles behave as rigid piles, while slender piles behave as flexible members.

Gupta and Basu [9] presented, in 2015, an analysis of a rigid monopile under various loading conditions. By considering the external forces acting on the monopile, they developed two sets of formulas to describe pile displacement and rotation. To evaluate the reliability of the developed formulas, they conducted a three-dimensional finite element analysis and found good agreement between the formula-based results and the numerical analysis.

Kim et al. [10], in 2016, studied the effect of monopile diameter on the relationship between lateral soil reaction, p, and pile deflection at a specific depth, y, commonly known as the p–y curve. Their results showed that pile diameter significantly affects the p–y curve. Accordingly, they concluded that special care should be taken when designing large-diameter monopiles. The use of p–y curves in designing monopiles in sandy soils is highly recommended by the American Petroleum Institute [11, 12]. Additionally, pile diameter and soil stratification were considered by Zachariah & Sahoo [13] in 2019 to study the behavior of a monopile tip under lateral loading. Their analysis was conducted using three-dimensional finite element modeling for piles installed in clay, sand, and multi-layered soils. Their results showed that as the diameter of a monopile increases, the pile tends to behave as a rigid member with minor deflection.

Byrne et al. [14] analyzed the results of field tests conducted on a monopile installed in over-consolidated glacial till under lateral loads. Tests were performed on three piles with diameters of 0.273 m, 0.762 m, and 2 m, and length-to-diameter ratios varying between 3 and 10. The data supported the development of a one-dimensional model to obtain a simplified monopile design. Their dataset is considered a unique source of information for piles installed in over-consolidated soils under lateral loads.

Raktate & Choudhary [15] conducted a parametric study in 2020 on a hollow monopile, focusing on water table variation and soil properties. By considering aerodynamic and hydrodynamic forces for various structural and soil parameters, a nonlinear static analysis of the substructure was performed. They proposed equations and nomographs applicable to similar environmental conditions and turbine characteristics, which reduce the time required for preliminary feasibility studies and simplify the design methodology.

Al-Qaisee et al. [16] in 2020 and Munaga & Gonavaram [17] in 2021 investigated the behavior of single piles and pile groups under lateral loads in sandy and multi-layered soils through a series of laboratory model tests. Their results showed that the tip deflection of both single piles and pile groups in multi-layered soils was less than that in sandy soils. In 2023, Yu et al. [18] examined the influence of sand anisotropy and scouring on a cyclically laterally loaded pile. The study was conducted through a series of model tests on monopiles with two cyclic load amplitudes, three soil deposition

angles, and two scour depths. They found that increasing the deposition angle of sand and scour depth increased the accumulated displacement at the pile head. Furthermore, sand anisotropy had a significant effect for piles under smaller cyclic amplitudes, whereas this effect was not observed for scouring.

Nanda et al. [19] in 2017 examined a monopile under uni-directional and multi-directional loadings. Their research, conducted under cyclic lateral loads, showed that multi-directional cyclic loading increased pile displacement and reduced pile stiffness compared with uni-directional loading. In 2024, Alsharedah et al. [20] investigated the performance of monopiles supporting a 5 MW wind turbine under horizontal loading using three-dimensional nonlinear finite element models. Various clayey soil profiles were included in the models. They found that soil strength and the ratio of embedment depth to pile diameter (L/D) significantly influenced monopile performance. As L/D increased, tower tip displacement decreased, while lateral capacity improved substantially.

Zhu et al. [21] studied the effects of reinforcements with different stiffness values, strengths, and reinforcement ranges on the lateral bearing capacity, deformations, soil resistance, and soil resistance per unit length relative to pile deflection (*p–y* curves) of monopiles using a finite element model. They found that, at the interface with unreinforced soil, the resistance provided by the reinforced soil decreased noticeably. Additionally, no significant change in the resistance of the unreinforced soil was observed due to the presence of the reinforced soil.

Haiderali et al. [22] published a study in 2024 to investigate the effect of loose sand layers (in terms of thickness and depth) on the monotonic lateral capacity of a 10 m diameter extra-large semi-rigid monopile loaded at an eccentricity of 36 m above the mudline in dense sand. A series of three-dimensional finite element analyses was carried out using the advanced SANISAND-04 constitutive model. They found that both the thickness and depth of the loose sand layer influenced the lateral capacity of the monopile. Additionally, reductions in bending moments and shear forces were observed due to the presence of loose layers. Moreover, the lateral capacity of monopiles was significantly affected when loose sand existed near the pile tip.

Menendez-Vicente et al. [23] conducted a new study in 2025 to investigate the beneficial effects of scour protection systems on offshore piled foundations. The study involved a parametric analysis of scour protection dimensions and materials and included both small-diameter and large-diameter monopiles. Numerical analysis using the finite element method was applied to evaluate natural frequencies and static capacity by employing both moment–lateral load (*M–H*) curves and the Load Utilization method. They found that rock fill improved the initial foundation conditions regardless of pile dimensions. Furthermore, scour protection achieved its dual objectives of preventing scour and increasing foundation stiffness for small-diameter monopiles, while its contribution to stiffness was limited for large-diameter monopiles. They also noted that scour protection should be further studied for heavy rock armor and significant protection heights.

He & Takahashi [24] in 2025 studied the seismic response of monopile-supported offshore wind turbines in sandy soil, considering the effects of soil–structure interaction (SSI), environmental loads, and soil liquefaction. The study was conducted using an advanced three-dimensional numerical soil model, and dynamic analyses were performed within the OpenSees framework. Their results highlighted the importance of higher vibration modes for large wind turbines and the significant role of SSI in dynamic response. Under the combined effects of wind, earthquake loading, and liquefaction, monopile-supported offshore wind turbines in dense sand experienced considerable lateral displacement and rotation. In the study, the monopile was subjected to a lateral displacement at the pile head equal to 10% of the pile diameter to examine both lateral and vertical deformations along the embedded pile length. The three-dimensional finite element software PLAXIS 3D was used to simulate a single layer of medium-dense sandy soil interacting with the monopile foundation. The study contributed to identifying the locations of zero lateral and vertical displacement along the embedded depth.

As mentioned earlier, monopiles are the most common type of foundation for offshore wind turbines, which are subjected to lateral loads from wind and water. In this study, the lateral and vertical displacements along the embedded length of a monopile foundation in sandy soil were investigated under a pile head lateral displacement equal to 10% of the monopile diameter. The ratio of monopile length in water to the embedded monopile length in soil (L/H) was considered, and the effects of monopile diameter (D) and monopile wall thickness (t) were also examined.

2. Modelling of Monopile-Soil System

The monopile embedment length in soil, *H*, was 20 m, while the water depth above the ground surface, *L*, was taken as 10 m and 20 m to achieve L/H ratios of 0.5 and 1.0, respectively. The selected monopile diameters (*D*) were 2.5 m and 5.0 m for both L/H ratios. The selected wall thicknesses were 1.5 mm and 3.0 mm for the two diameters and L/H ratios. Figure 1 summarizes the workflow chart. Table 1 presents the monopile properties, and Figure 2 shows a schematic representation of the monopile model together with the soil layer.

The soil depth was 40 m to eliminate boundary effects and consisted of a single layer of medium-dense sand. Soil characteristics are shown in Table 2. A ten-noded tetrahedral element was used in the computational analyses. The sandy

layer was modeled as medium dense, and the soil behavior was simulated using the Mohr–Coulomb model under drained conditions. The dilatancy angle for the sandy soil was set to 7.0°, depending on soil density and internal friction angle.

The modeling was performed in two stages. The first stage simulated the installation of the monopile, and the second stage applied lateral displacement. The global mesh coarseness factor was 0.5, while a finer coarseness factor of 0.25 was used around the monopile and the surrounding soil. To examine the lateral and vertical deformations along the embedded length of the monopile, a lateral displacement equal to 10% of the monopile diameter (*D*) was applied at the pile head.

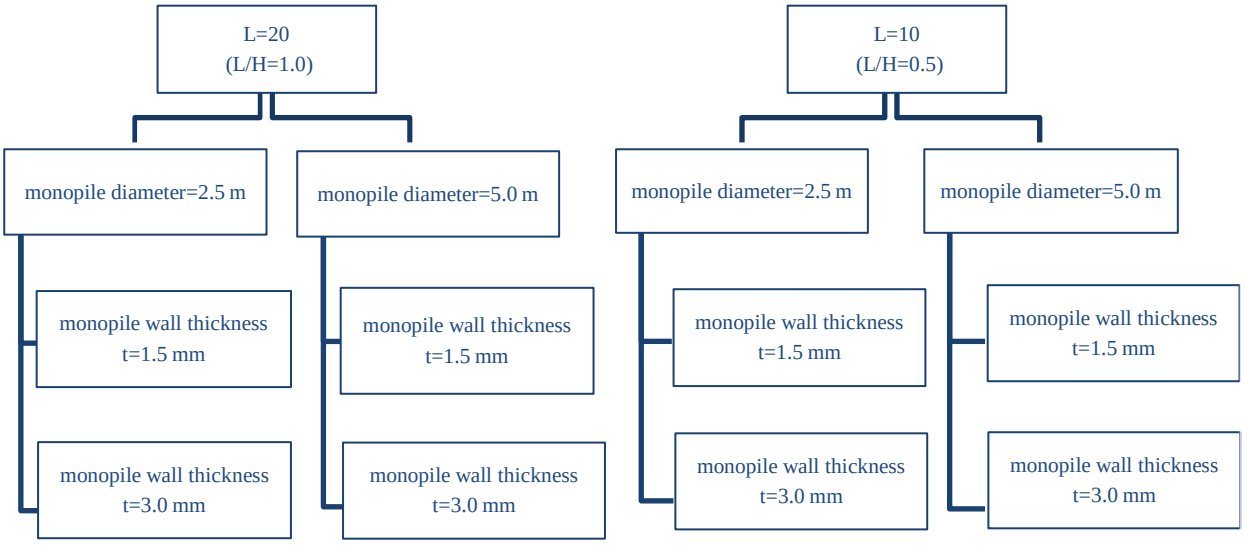

Figure 1. The flow chart of workflow

Table 1. Properties of monopile wall

Parameter	Name	Value	
Identification	-	t_1	t_2
Thickness, mm	T	15	30
Unit weight, kN/m^3	Γ	78.00	78.00
Stiffness, kN/m^2	E_1	200*10^6	200*10^6
	E_2	200*10^6	200*10^6
	N	0.15	0.15

Table 2. Characteristics of sand used in modelling

Parameter	Name	Value
Material used	Model	Mohr-Coulomb
Type of analysis	Type	Drained
Soil unit weight, kN/m^3	γ	18.70
Initial void ratio	e_o	0.60
Stiffness, kN/m^2	E	25000
	ν	0.25
Cohesion, kN/m^2	C_{ref}	15.0
Angle of internal friction, degrees	ϕ	37.0
Dilatancy angle	ψ	7.0
R inter	-	0.7
Data set	-	USDA
Model	-	Van Genuchten

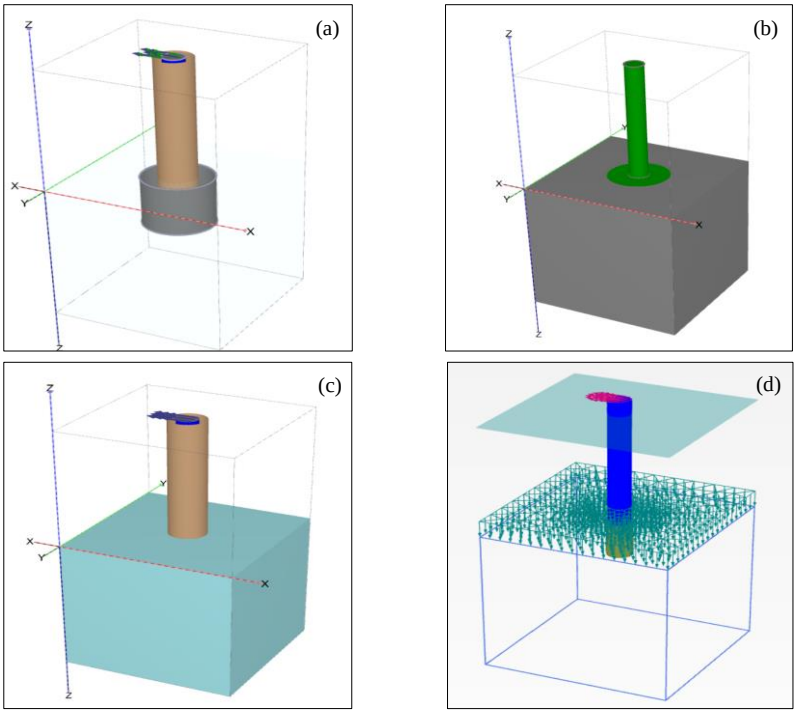

Figure 2. Schematic representation of modeling monopile and soil layers

3. Results and Discussion

PLAXIS 3D software was used for the simulations through a series of three-dimensional finite element analyses. The lateral displacement (U_x) was examined along the total monopile depth, considering the effect of diameter at constant wall thickness for each L/H ratio. Comparisons were also made between wall thicknesses for the two selected diameters. In addition, the vertical displacement (U_z) of the monopile was examined along the depth for different diameters, wall thicknesses, and L/H ratios. The variation of the points where the lateral displacement became zero (inflection points), L_{Hzero}, within the sandy layer was also studied.

3.1. Effect of Monopile Thickness and Diameter on Embedded Depth of Lateral Displacement

Figures 3(a) and 3(b) illustrate the comparative analysis of lateral displacement along the monopile length for wall thicknesses of 1.5 mm and 3.0 mm for each diameter (2.5 m and 5.0 m) when L/H = 1. In general, the behavior was similar for both diameters and thicknesses. However, the depth at which lateral displacement approached zero (L_{Hzero}) increased with increasing monopile diameter and thickness. The value of L_{Hzero} increased from 3.057 m to 4.312 m for a wall thickness of 1.5 mm, and from 8.361 m to 10.185 m for a wall thickness of 3.0 mm. The lateral displacement at the interface between sand and water (D_{Lzero}) also increased with increasing monopile diameter. It increased from 25.30 mm to 30.18 mm for a wall thickness of 1.5 mm, and from 37.12 mm to 53.51 mm for a wall thickness of 3.0 mm, as the diameter increased from 2.5 m to 5.0 m. The results for different monopile diameters showed good agreement with those reported by Kim et al. [10] and Ji et al. [25], confirming the reliability of the lateral displacement trends.

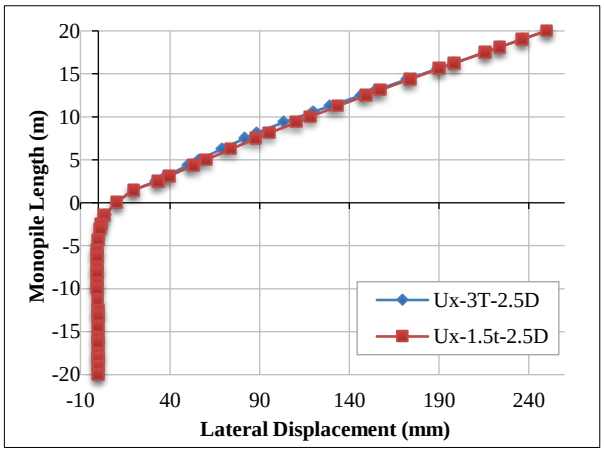

(a) lateral displacement along monopile of 2.5 m diameter and L/H = 1

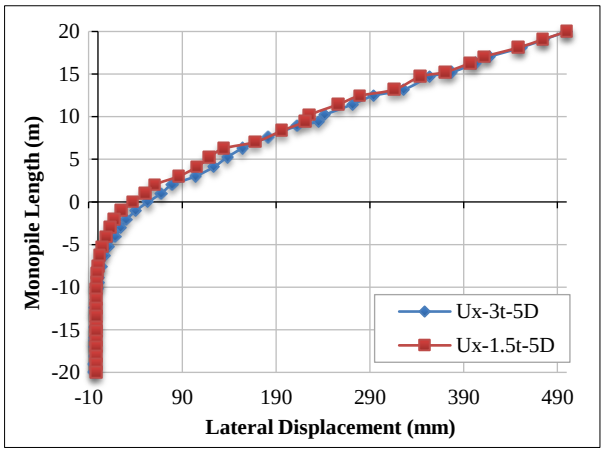

(b) lateral displacement along monopile of 5.0 m diameter and L/H = 1

Figure 3. Variation of embedded depth of lateral displacement along monopile length for L/H =1.0 and different monopile-wall thicknesses and diameters

Figures 4(a) and 4(b) present a comparative analysis of lateral displacement along the monopile length for wall thicknesses of 1.5 mm and 3.0 mm for both diameters (2.5 m and 5.0 m) when L/H = 0.5. The value of L_{Hzero} varied from 5.00 m to 8.00 m for a wall thickness of 1.5 mm, and from 8.00 m to 10.916 m for a wall thickness of 3.0 mm. The lateral displacement at the sand–water interface (D_{Lzero}) increased with increasing diameter. It increased from 25.61 mm to 33.00 mm for a wall thickness of 1.5 mm, and from 95.5 mm to 138.5 mm for a wall thickness of 3.0 mm, as the diameter increased from 2.5 m to 5.0 m.

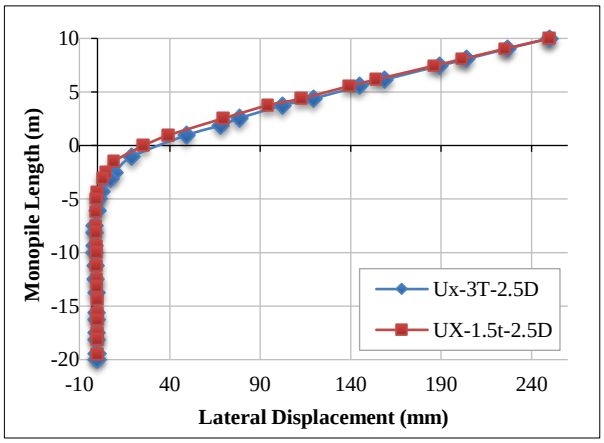

(c) lateral displacement along monopile of 2.5 m diameter and L/H = 0.5

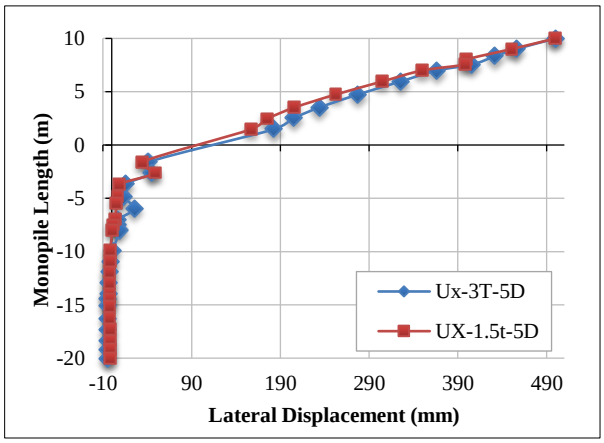

(d) lateral displacement along monopile of 5.0 m diameter and L/H = 0.5

Figure 4. Variation of embedded depth of lateral displacement along monopile length for L/H =0.5 and different monopile-wall thicknesses and diameters

The lateral displacement along the monopile length is illustrated in Figures 5 and 6 for L/H = 1 and L/H = 0.50, respectively. These figures analyze the variation in lateral displacement for wall thicknesses of 1.5 mm and 3.0 mm for each diameter.

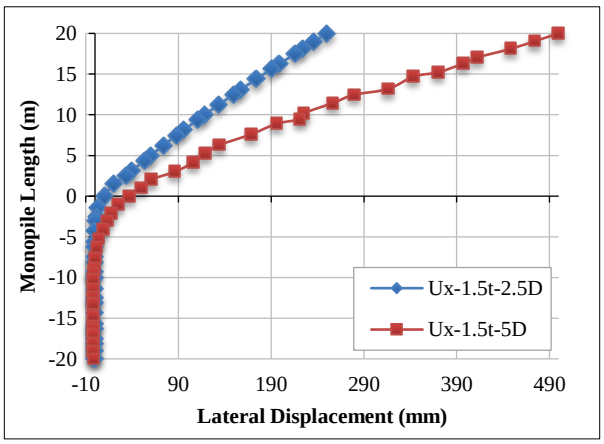

(a) lateral displacement along monopile length of 1.5 mm wall thickness

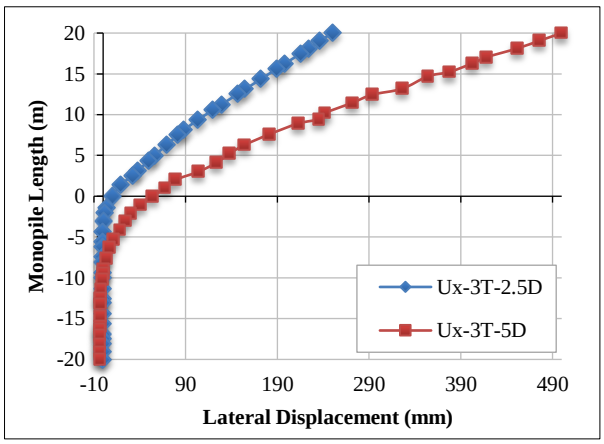

(b) lateral displacement along monopile length of 3 mm wall thickness

Figure 5. Variation of lateral displacement along monopile length for L/H = 1

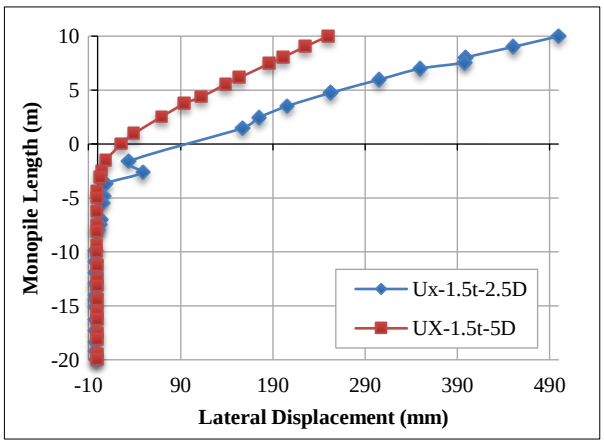

(a) lateral displacement along monopile of 1.5 mm wall thickness and L/H = 0.5

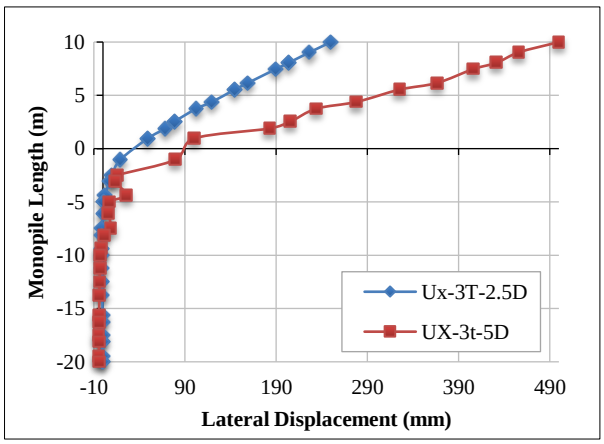

(b) lateral displacement along monopile of 3 mm wall thickness and L/H = 0.5

Figure 6. Variation of lateral displacement along monopile length for L/H = 0.5

For L/H = 1, it can be observed that the value of L_{Hzero} increased from 3.057 mm to 8.361 mm when the wall thickness was kept constant at 1.5 mm. Similarly, L_{Hzero} increased from 4.312 mm to 10.185 mm when the wall thickness was set at 3.0 mm. In addition, the lateral displacement of the monopile at the boundary between sand and water (D_{Lzero}) showed a significant increase as the monopile diameter increased, regardless of wall thickness. Specifically, D_{Lzero} increased from 25.30 mm to 37.12 mm for a thickness of 1.5 mm, and from 30.18 mm to 53.51 mm for a thickness of 3.0 mm, as the diameter increased from 2.5 m to 5.0 m.

For L/H = 0.5, the value of L_{Hzero} varied between 5.00 mm and 8.00 mm for a wall thickness of 1.5 mm, and between 7.50 mm and 10.916 mm for a wall thickness of 3.0 mm. The lateral displacement at the sand–water boundary (D_{Lzero}) also increased as the diameter increased. It rose from 25.61 mm to 33.00 mm for a wall thickness of 1.5 mm, and from 95.5 mm to 138.5 mm for a wall thickness of 3.0 mm, corresponding to a diameter increase from 2.5 m to 5.0 m.

In this manner, the embedded depth at which lateral displacement becomes zero increases with increasing diameter; however, this increase is smaller for thinner wall sections compared to thicker ones. Furthermore, as the monopile diameter decreases, the pile behaves more like a flexible pile, and the deflection at the pile head becomes larger. Table 3 presents the embedded depth of zero lateral displacement (L_{Hzero}) for different wall thicknesses and L/H ratios.

Table 3. The embedded depth of zero lateral displacement, L_{Hzero}, and the lateral displacement D_{Lzero} for different wall thicknesses and L/H ratios

Diameter, D, (m)	L/H	Wall thickness, W (mm)	Pile Rigidity, EI (kN.m^2)	Embedded depth of zero lateral displacement, L_{Hzero}, (m)	Lateral displacement value of the monopile at the boundary between the sand and water, DLzero,
2.5	1	3.00	3.727×10^6	4.312	30.18
		1.50	2.522×10^6	3.057	25.00
5.0	1	3.00	8.247×10^6	10.185	53.51
		1.50	1.855×10^7	8.361	37.12
2.5	0.5	3.00	-	7.500	33.00
		1.50		5.002	25.61
5.0	0.5	3.00	-	10.916	95.50
		1.50		8.000	138.5

In general, the behavior was identical for both diameters and wall thicknesses; however, the depth at which the lateral displacement approached zero (L_{Hzero}) increased with larger monopile diameters and thicker walls. The point of L_{Hzero} represents the pile center in the upper part of the embedded length, where the pile is subjected to forces resulting from the applied external lateral displacement. Below this point, the pile compresses the surrounding soil, and this behavior is influenced by soil–structure interaction.

The flexural rigidity (EI) of the pile increased significantly as both the diameter and wall thickness increased. As a result, the pile became more rigid and exhibited greater resistance to bending, causing the location of L_{Hzero} to move downward. This increase in lateral resistance highlights the significant impact of monopile diameter on structural stability. As the diameter increases, resistance to lateral forces improves, making it essential to consider these factors in the design process.

When the L/H ratio increased from 0.50 to 1.0 (indicating a doubling of the water height) under constant wall thickness, the parameter L_{Hzero} decreased. This reduction was more pronounced for the 2.5 m diameter pile, whereas the 5.0 m diameter pile showed negligible response regardless of wall thickness. The 5.0 m diameter pile, with both wall thicknesses considered, exhibited substantial rigidity, and variations in the L/H ratio did not significantly affect its behavior or the location of L_{Hzero}, even though the overturning moment caused by water pressure was effectively reduced by half. In contrast, the 2.5 m diameter pile, with both wall thicknesses, demonstrated greater flexibility and showed a noticeable reduction in L_{Hzero} as the L/H ratio increased.

This highlights an important principle in geotechnical engineering: increasing pile diameter enhances stability but reduces the system's flexibility in responding to changing load conditions.

3.2. Effect of Monopile-Wall Thickness and Diameter on the Embedded Depth of Vertical Displacement

The variation of vertical displacement along the total embedded depth of monopiles with diameters of 2.5 m and 5.0 m is presented in Figures 7-a and 7-b for an L/H ratio of 1, and in Figures 7-c and 7-d for an L/H ratio of 0.5, for the same diameters and wall thicknesses. In general, the vertical displacement of the monopile decreased with increasing depth until it reached a stable condition at the pile tip. Skin friction at the interface between the monopile surface and the surrounding soil increased with depth, providing resistance that prevented further settlement; consequently, vertical displacement decreased with depth.

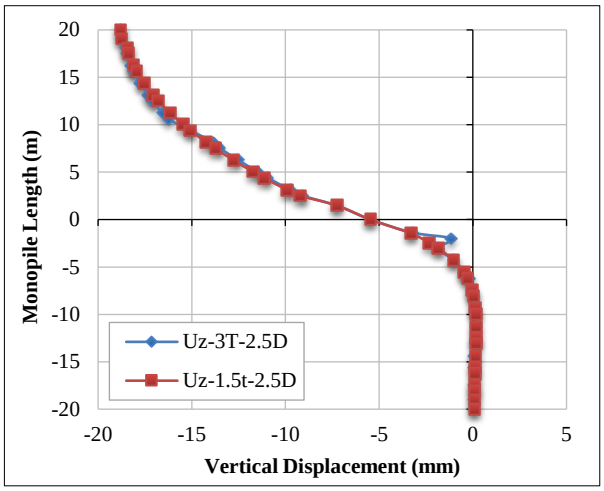

(a) Vertical displacement along monopile of 2.5 m diameter and L/H = 1

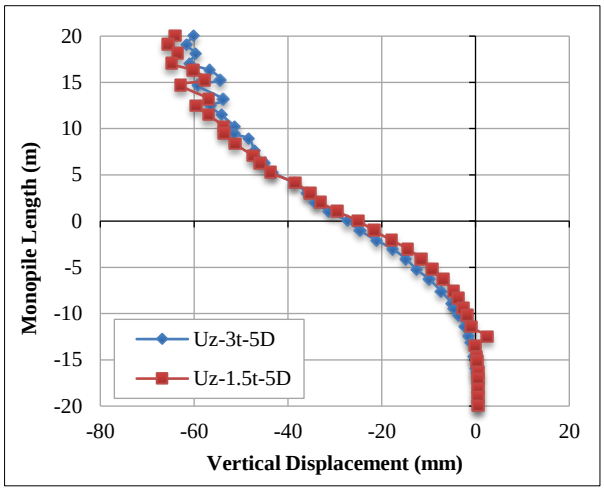

(b) Vertical displacement along monopile of 5.0 m diameter and L/H = 1

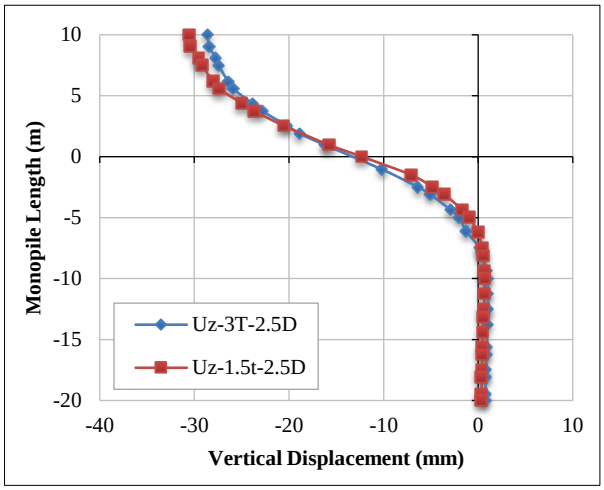

(c) Vertical displacement along monopile of 2.5 m diameter and L/H = 0.5

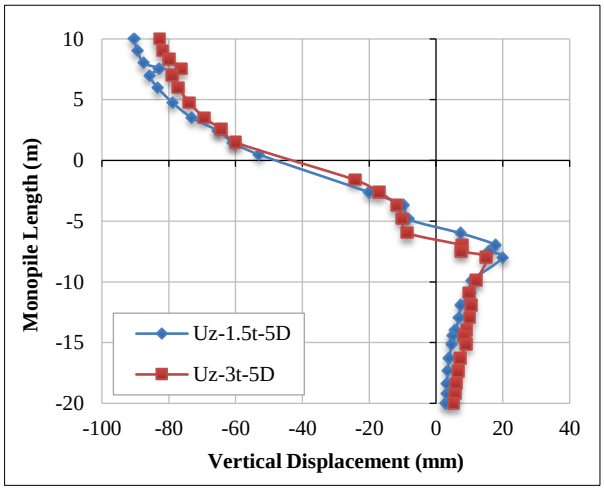

(d) Vertical displacement along monopile of 5.0 m diameter and L/H = 0.5

Figure 7. Variation of vertical displacement along monopile length for different diameters and thicknesses

It can be noted that the depth associated with zero vertical displacement, L_{Vzero}, increased for wall diameters of 2.5 m and 5 m, while showing minimal influence from changes in wall thickness. In summary, it can be concluded that no direct relationship exists between wall thickness and the embedded depth at which zero vertical displacement occurs. In addition, the depth corresponding to zero vertical displacement, L_{Vzero}, decreased as the L/H ratio was reduced, with a more pronounced decrease observed for larger diameters. Table 4 illustrates the depth at which zero vertical displacement, L_{Vzero}, occurs for different wall thicknesses and L/H ratios, and also presents the maximum vertical displacement at the monopile head. Under constant wall thickness and monopile diameter, an increase in the L/H ratio is associated with an increase in maximum vertical displacement due to the monopile's rigidity; as the monopile diameter increases, its behavior more closely resembles that of a rigid structural element.

Table 4. The embedded depth of zero vertical displacement, L_{Hzero}, for different wall thicknesses and L/H ratios

Diameter, D (m)	L/H	Wall thickness, W (mm)	Embedded depth of zero vertical displacement, L_{Vzero}, (m)	Maximum vertical displacement, Uz, at pile head
2.5	1	3.00	-8.101	-18.790
		1.50	-8.101	-18.781
5.0	1	3.00	-14.711	-60.093
		1.50	-14.711	-63.897
2.5	0.5	3.00	-7.500	-28.588
		1.50	-7.500	-30.569
5.0	0.5	3.00	-5.603	-82.622
		1.50	-5.600	-90.349

It can also be observed that the depth of zero vertical displacement, denoted as L_{Vzero}, increased with diameters of 2.5 m and 5 m; however, this variation had a negligible effect on wall thickness. In other words, a direct correlation between wall thickness and the embedded depth corresponding to zero vertical displacement does not exist. Furthermore, L_{Vzero} decreased as the L/H ratio decreased, with a more pronounced reduction occurring for larger diameters. Table 4 presents the embedded depth of zero vertical displacement, L_{Vzero}, for various wall thicknesses and L/H ratios, and shows the maximum vertical displacement at the monopile head. It has been noted that for constant monopile wall thickness and diameter, an increase in the L/H ratio leads to an increase in maximum vertical displacement, which can be attributed to the rigidity of the monopile. As the monopile diameter increases, it tends to behave more like a rigid structural component. Figures 8 and 9 show the variation of lateral and vertical displacement based on numerical results.

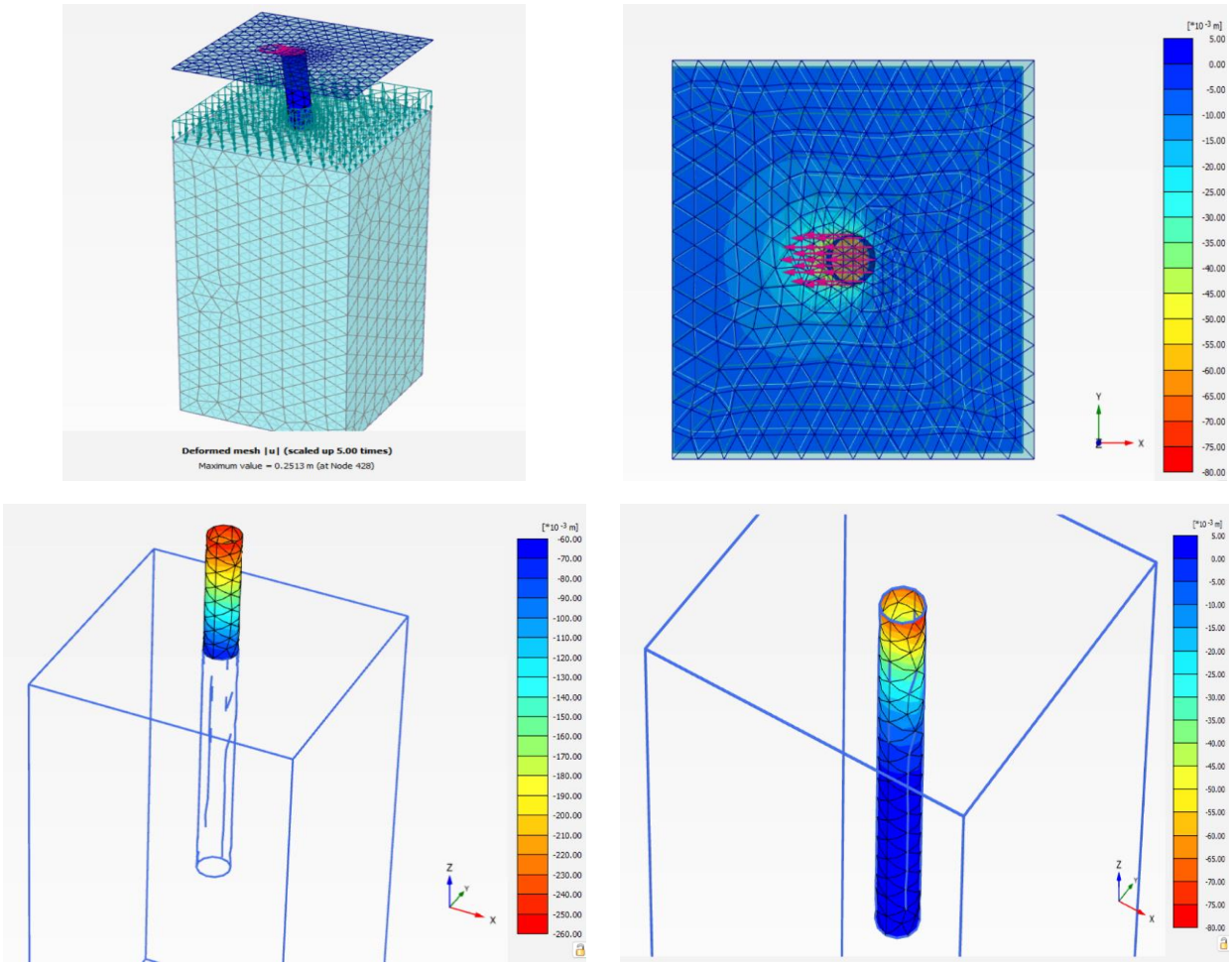

Figure 8. the variation of Lateral Displacement by Numerical Outputs

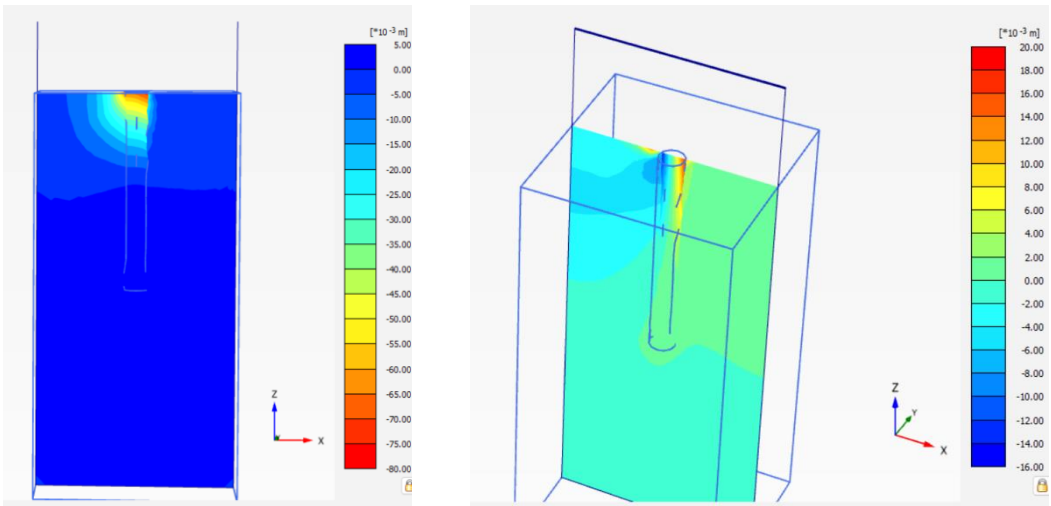

Figure 9. the variation of Vertical Displacement by Numerical Outputs

4. Conclusions

The following conclusions can be drawn from the foregoing analysis:

- The variation of lateral displacement with depth shows a consistent trend regardless of pile thickness or diameter. However, due to pile rigidity, the depth of zero lateral displacement, L_{Hzero}, varies. The embedded depth of zero lateral displacement, L_{Hzero}, decreases as monopile wall thickness decreases, but the magnitude of reduction for small diameters is greater than that for large diameters, regardless of the L/H ratio.
- The effect of increasing the L/H ratio on the embedded depth of zero lateral displacement, L_{Hzero}, diminishes as monopile diameter increases for the same wall thickness. The influence of L/H variation on L_{Hzero} increases for a monopile with a diameter of 2.5 m and wall thicknesses of 1.5 mm and 3 mm by 64% and 74%, respectively, for L/H ratios of 1.0 and 0.5. Meanwhile, for a monopile with a 5 m diameter, the increase did not exceed 10%. Moreover, for L/H = 1.0, when the monopile wall thickness decreased by 50%, the embedded depth of zero lateral displacement decreased by 29% and 18% for pile diameters of 2.5 m and 5 m, respectively. For L/H = 0.5, when the monopile wall thickness decreased by 50%, the embedded depth of zero lateral displacement decreased by 33% and 27% for pile diameters of 2.5 m and 5 m, respectively.
- The effect of monopile diameter on vertical displacement shows that as the monopile diameter increases, the depth of zero vertical displacement decreases. Also, as the L/H ratio decreases, the depth of zero vertical displacement declines. Monopile wall thickness has a negligible effect on vertical pile displacement.

5. List of Symbols

D = diameter of monopile, m.

H= embedded monopole depth in soil, m.

L= embedded monopole depth in water, m.

L_{Hzero} = embedded depth at which the zero of lateral displacement from ground level, m.

L_{Vzero} = embedded depth of zero vertical displacement, m.

$D_{Lzero=}$ lateral displacement of monopile at borderline between the sand and water.

t = thickness of the wall of the monopile, mm.

U_x = lateral displacement, mm.

U_z = vertical displacement, mm

6. Declarations

6.1. Author Contributions

Conceptualization, A.G. and N.F.; methodology, A.G. and N.F.; software, A.G.; validation, A.G., N.F., and M.Z.; formal analysis, M.Z.; investigation, N.F.; resources, N.F.; data curation, A.G.; writing—original draft preparation, M.Z.; writing—review and editing, A.G.; visualization, A.G.; supervision, M.Z.; project administration, A.G. and M.Z.; funding acquisition, N.F. and M.Z. All authors have read and agreed to the published version of the manuscript.

6.2. Data Availability Statement

The data presented in this study are available on request from the corresponding author.

6.3. Funding

The authors received no financial support for the research, authorship, and/or publication of this article.

6.4. Conflicts of Interest

The authors declare no conflict of interest.

7. References

[1] Hou, G., Xu, K., & Lian, J. (2022). A review on recent risk assessment methodologies of offshore wind turbine foundations. Ocean Engineering, 264, 103–119. doi:10.1016/j.oceaneng.2022.112469.

[2] Kozubal, J., Puła, W., Wyjadłowski, M., & Bauer, J. (2013). Influence of varying soil properties on evaluation of pile reliability under lateral loads. Journal of Civil Engineering and Management, 19(2), 272–284. doi:10.3846/13923730.2012.756426.

[3] Luo, R., Wang, A., Li, J., Ding, W., & Zhu, B. (2024). Simplified Design Method of Laterally Loaded Rigid Monopiles in Cohesionless Soil. Journal of Marine Science and Engineering, 12(2), 208. doi:10.3390/jmse12020208.

[4] Yang, M., Luo, R., & Li, W. (2018). Numerical study on accumulated deformation of laterally loaded monopiles used by offshore wind turbine. Bulletin of Engineering Geology and the Environment, 77(3), 911–921. doi:10.1007/s10064-017-1138-9.

[5] Zhang, L. (2009). Nonlinear analysis of laterally loaded rigid piles in cohesionless soil. Computers and Geotechnics, 36(5), 718–724. doi:10.1016/j.compgeo.2008.12.001.

[6] Higgins, W., Vasquez, C., Basu, D., & Griffiths, D. V. (2013). Elastic Solutions for Laterally Loaded Piles. Journal of Geotechnical and Geoenvironmental Engineering, 139(7), 1096–1103. doi:10.1061/(asce)gt.1943-5606.0000828.

[7] Haiderali, A., Cilingir, U., & Madabhushi, G. (2013). Lateral and Axial Capacity of Monopiles for Offshore Wind Turbines. Indian Geotechnical Journal, 43(3), 181–194. doi:10.1007/s40098-013-0056-4.

[8] Lada, A., Gres, S., Nicolai, G., & Ibsen, L. B. (2014). Response of a stiff monopile for a long-term cyclic loading. DCE Technical Memorandum, Department of Civil Engineering, Aalborg University, Aalborg, Denmark.

[9] Kumar Gupta, B., & Basu, D. (2015). Analysis of offshore wind turbine rigid Monopile Foundation. From Fundamentals to Applications in Geotechnics, IOS Press, Amsterdam, Netherlands. doi:10.3233/978-1-61499-603-3-822.

[10] Kim, D., Choo, Y. W., Park, J. H., & Kwak, K. (2016). Review of offshore monopile design for wind turbine towers. Japanese Geotechnical Society Special Publication, 4(7), 158–162. doi:10.3208/jgssp.v04.k10.

[11] American Petroleum Institute (API). (2011). Geotechnical and Foundation Design Considerations. API RP 2GEO, American Petroleum Institute (API), Washington, United States.

[12] Wang, H., Lehane, B. M., Bransby, M. F., Wang, L. Z., Hong, Y., & Askarinejad, A. (2023). Lateral behavior of monopiles in sand under monotonic loading: Insights and a new simple design model. Ocean Engineering, 277. doi:10.1016/j.oceaneng.2023.114334.

[13] Zachariah, J. P., & Sahoo, J. P. (2021). Response of Laterally Loaded Monopile Using Three-Dimensional Finite Element Analysis. Proceedings of the Indian Geotechnical Conference 2019, Lecture Notes in Civil Engineering, Springer, Singapore. doi:10.1007/978-981-33-6346-5_34.

[14] Byrne, B. W., McAdam, R. A., Burd, H. J., Beuckelaers, W. J. A. P., Gavin, K. G., Houlsby, G. T., Igoe, D. J. P., Jardine, R. J., Martin, C. M., Muirwood, A., Potts, D. M., Gretlund, J. S., Taborda, D. M. G., & Zdravkovic, L. (2020). Monotonic laterally loaded pile testing in a stiff glacial clay till at Cowden. Geotechnique, 70(11), 970–985. doi:10.1680/jgeot.18.PISA.003.

[15] Raktate, T., & Choudhary, R. (2020). Design of Monopile Foundation for Offshore Wind Turbine. E3S Web of Conferences, 170. doi:10.1051/e3sconf/202017001024.

[16] Al-Qaisee, G. S., Ahmed, M. D., & Ahmed, B. A. (2020). Performance of piled raft foundations under the effect of dewatering nearby an open pit. IOP Conference Series: Materials Science and Engineering, 737(1), 737. doi:10.1088/1757-899X/737/1/012081.

[17] Munaga, T., & Gonavaram, K. K. (2021). Influence of Stratified Soil System on Behavior of Laterally Loaded Pile Groups: An Experimental Study. International Journal of Geosynthetics and Ground Engineering, 7(2), 18. doi:10.1007/s40891-021-00263-0.

[18] Yu, F., Zhang, C., Huang, M., Yang, X., & Yao, Z. (2023). Model Tests on Cyclic Responses of a Laterally Loaded Pile Considering Sand Anisotropy and Scouring. Journal of Marine Science and Engineering, 11(2), 255. doi:10.3390/jmse11020255.

[19] Nanda, S., Arthur, I., Sivakumar, V., Donohue, S., Bradshaw, A., Keltai, R., Gavin, K., Mackinnon, P., Rankin, B., & Glynn, D. (2017). Monopiles subjected to uni- and multi-lateral cyclic loading. Proceedings of the Institution of Civil Engineers: Geotechnical Engineering, 170(3), 246–258. doi:10.1680/jgeen.16.00110.

[20] Alsharedah, Y., Newson, T., & El Naggar, M. H. (2024). A 3-D modelling of monopile behaviour under laterally applied loading. Geomechanics and Geophysics for Geo-Energy and Geo-Resources, 10(1), 173. doi:10.1007/s40948-024-00874-7.

[21] Zhu, T., He, R., & Guo, Z. (2024). Numerical simulation of offshore monopiles with reinforcement in shallow soil layer. IOP Conference Series: Earth and Environmental Science, 1337(1), 12069. doi:10.1088/1755-1315/1337/1/012069.

[22] Haiderali, A. E., & Madabhushi, G. S. P. (2025). Effect of loose sand layers within dense sand on the lateral capacity of extra-extra-large monopiles. Marine Georesources and Geotechnology, 43(7), 1324–1338. doi:10.1080/1064119X.2024.2405160.

[23] Menéndez-Vicente, C., López-Querol, S., Harris, J. M., & Tavouktsoglou, N. S. (2025). Numerical study on the stiffening properties of scour protection around monopiles for Offshore Wind Turbines. Engineering Geology, 345, 107835. doi:10.1016/j.enggeo.2024.107835.

[24] He, W., & Takahashi, A. (2025). Dynamic response analysis of monopile-supported offshore wind turbine on sandy ground under seismic and environmental loads. Soil Dynamics and Earthquake Engineering, 189, 109105. doi:10.1016/j.soildyn.2024.109105.

[25] Ji, J., Lin, Z., Li, S., Song, J., & Du, S. (2024). Coupled Newmark seismic displacement analysis of cohesive soil slopes considering nonlinear soil dynamics and post-slip geometry changes. Computers and Geotechnics, 174, 106628. doi:10.1016/j.compgeo.2024.106628.